

National Aeronautics and Space Administration

ASCA GUEST INVESTIGATOR PROGRAM

ANNUAL STATUS REPORT FOR NAG 5-2524

Submitted by: The Trustees of Columbia University  
in the City of New York  
351 Engineering Terrace  
New York, New York 10027

Prepared by: Columbia Astrophysics Laboratory  
Departments of Astronomy and Physics  
Columbia University  
538 West 120<sup>th</sup> Street  
New York, New York 10027

Principal Investigator: Jules P. Halpern  
Associate Professor of Astronomy

Title of Research: "X-Ray Spectrum of a Narrow Line  
Quasi-Stellar Object"

Period Covered by Report: 15 March 1994 – 14 March 1996

April 1996

## TABLE OF CONTENTS

|                                                  |   |
|--------------------------------------------------|---|
| 1. X-ray Spectrum of a Narrow-Line QSO . . . . . | 1 |
| 2. The Geminga Pulsar . . . . .                  | 4 |
| 3. Warm Absorbers: The Moment of Truth . . . . . | 6 |
| REFERENCES . . . . .                             | 9 |

## 1. X-ray Spectrum of a Narrow-Line QSO

This AO-3 observation of a new narrow-line QSO was motivated by our extensive study (Moran, Halpern, & Helfand 1994,1996) of the unclassified X-ray sources from the *ROSAT/IRAS* all-sky survey of Boller *et al.* (1992). The object designated IRAS 2018.1–2244 was observed by Elizalde & Steiner (1994) and by us with higher quality spectroscopy (see Figure 1) to have Balmer lines and forbidden lines of roughly equal width,  $700 \text{ km s}^{-1}$  FWHM. There are possibly weak broad wings on the  $\text{H}\alpha$  line. One of the questions to be addressed by hard X-ray spectroscopy is whether or not these wings are to be interpreted as scattered or weakly transmitted flux from a hidden broad-line region. The optical spectrum of IRAS 2018.1–2244 also has very weak permitted Fe II lines (Moran *et al.* 1996). This feature is possibly indicative of a hidden broad line region, as it is also seen in the prototypical hidden Seyfert 1 galaxy NGC 1068. At a redshift of 0.185, IRAS 2018.1–2244 has a 0.1–2.4 keV X-ray luminosity of  $4 \times 10^{44} \text{ ergs s}^{-1}$ . A hard X-ray spectrum obtained by *ASCA* would be the primary means by which one could determine if obscuration is preventing us from viewing the nucleus directly.

A new wrinkle on the concept of the narrow-line QSO is the gradual realization that luminous objects with very strong but narrow Fe II lines are showing up preferentially in soft X-ray surveys. Many of these should be grouped with the well-known prototype I Zw 1 (Phillips 1976), which itself has been called a narrow-line QSO according to criteria of luminosity and line width. One of the first and most luminous such objects to be detected in X-rays was the *HEAO* 1 source PKS 0558–504. Its optical line widths are  $1500 \text{ km s}^{-1}$ , and its 2–10 keV X-ray luminosity is  $2.5 \times 10^{45} \text{ ergs s}^{-1}$  (Remillard *et al.* 1986). This X-ray source further distinguished itself by emitting a super-Eddington flare in a subsequent *Ginga* observation (Remillard *et al.* 1991). Indeed, it is now apparent that the I Zw 1 class are strong soft X-ray sources with steep spectra that are prone to rapid and large amplitude variability. Other examples are RX 1322.4–3809 (Boller *et al.* 1993), Arakelian 564 (Brandt *et al.* 1994), and IC 3599 (Brandt *et al.* 1995; Grupe *et*

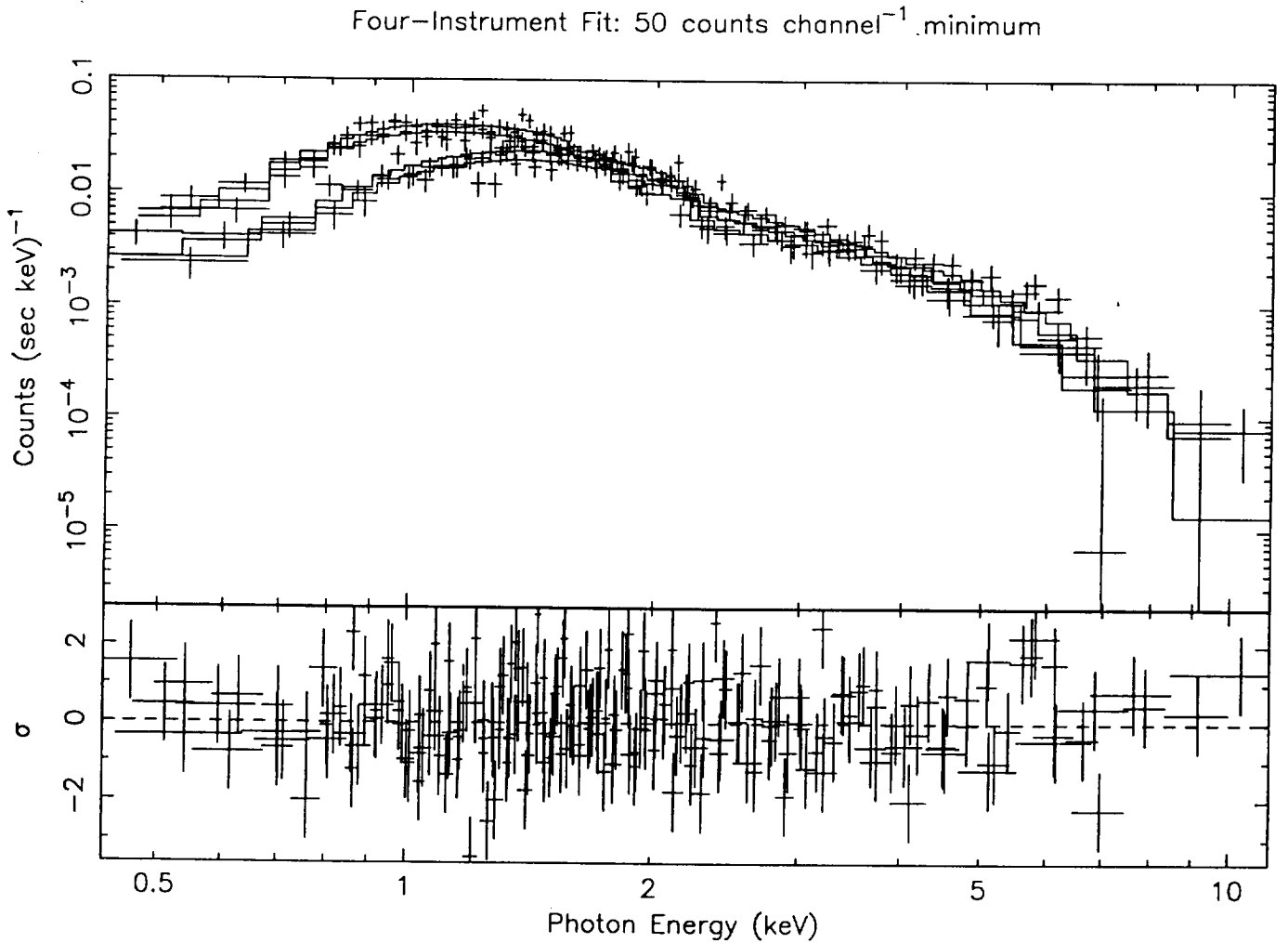


FIG. 1.— Power-law fit to the *ASCA* spectra of IRAS 2018.1-2244 in all four instruments simultaneously.

*al.* 1995). So for these objects, at least, the soft X-ray spectrum and rapid variability are good indicators that we are seeing directly into the nucleus, and that the observed ionizing continuum is representative of its intrinsic luminosity. Since the optical spectrum of IRAS 2018.1-2244 has weak Fe II lines, it might be a I Zw 1 object, and not a hidden QSO at all.

A 60 ksec observation of IRAS 2018.1-2244 was performed in 1995 October, and we have the following preliminary results from a simultaneous fit to all four detectors, as illustrated in Figures 1 and 2. The photon spectral index is  $2.38 \pm 0.07$ . The column density,  $(2.9 \pm 0.4) \times 10^{21} \text{ cm}^{-2}$ , is significantly larger than the Galactic value of  $7.4 \times 10^{20} \text{ cm}^{-2}$ , but

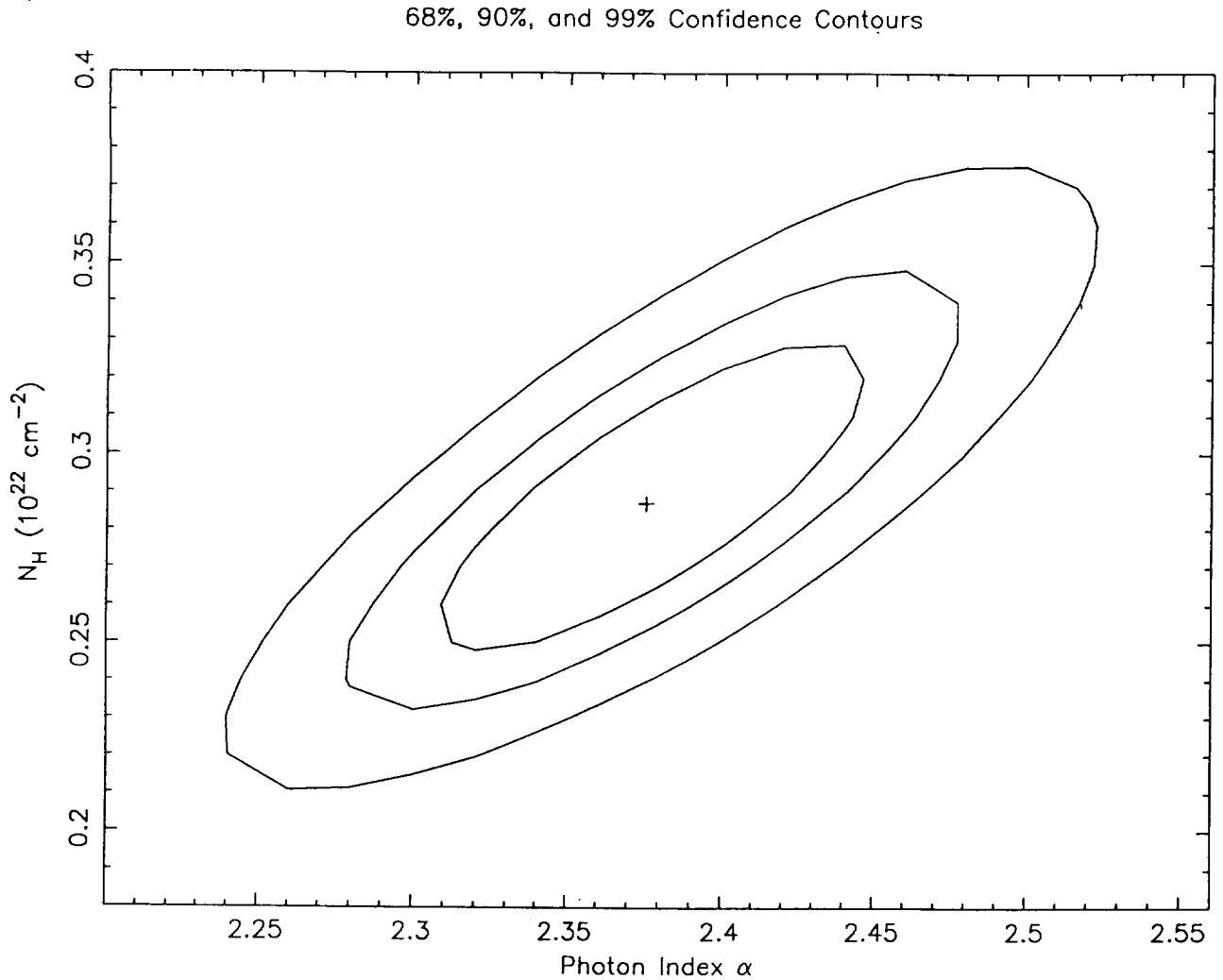


FIG. 2.— Confidence contours for the spectral parameters in the power-law fit to IRAS 2018.1–2244 shown in Figure 1.

not indicative of large obscuration. The X-ray luminosity in the intrinsic 2–10 keV band is  $2.8 \times 10^{44}$  ergs s $^{-1}$ . If extrapolated into the *ROSAT* band, these spectral parameters would predict an X-ray flux approximately four times as large as that observed by Boller *et al.* (1992). The implied variability would argue against a scattering interpretation from a hidden nucleus. There is also a hint of an Fe K $\alpha$  line in the spectrum, which we are continuing to investigate. However, the preliminary results of the analysis of the continuum are more consistent with an unobscured I Zw 1 object than with a hidden QSO.

## 2. The Geminga Pulsar

The high-energy  $\gamma$ -ray source “Geminga” is a rotation-powered pulsar with period  $P = 0.237$  s, surface magnetic field  $B_p \sim 1.6 \times 10^{12}$  G, and spin-down age  $\tau = P/2\dot{P} = 3.4 \times 10^5$  yr (Halpern & Holt 1992; Bertsch et al. 1992). It is the only radio-quiet pulsar known. Geminga has injected new life into several key problems in high-energy astrophysics. Among these are *a)* the physics of particle acceleration in pulsars, *b)* the interpretation of the unidentified  $\gamma$ -ray sources in the Galactic plane, and *c)* the study of thermal X-ray emission from neutron star photospheres. Although Geminga is a strong soft X-ray and  $\gamma$ -ray source, it has not yet been studied in the standard 2–10 keV window of classical X-ray astronomy, apparently falling below the thresholds of previous, non-imaging instruments. The principal objectives of this AO-1 observation were to detect Geminga and to interpret its 2–10 keV spectrum and pulse profile in terms of the following questions:

- (a) Are the hard X-rays an extrapolation of the double-pulsed  $\gamma$ -ray beams, the tail of the soft thermal X-ray emission, or a completely new component waiting to be discovered?
- (b) Is the harder of the two components clearly seen in the *ROSAT* X-ray spectrum of Geminga thermal (blackbody) emission from a heated polar cap region, or synchrotron radiation from the inner magnetosphere? The *ROSAT* data alone cannot distinguish between these two models, but the *combination* of *ROSAT* and *ASCA* spectra can easily do so. Heating of the polar caps by particles flowing inward on the open field lines is our favored interpretation, and a by-product to varying degrees of all models of magnetosphere accelerators which produce  $\gamma$ -rays (Ruderman & Sutherland 1975; Arons 1981; Harding et al. 1993; Halpern & Ruderman 1993). This is one of the principal observations which can test these models.
- (c) If the hard component is polar cap emission, what is its temperature, emitting area, and geometry? The X-ray pulse profile can be used to constrain the geometry of the surface magnetic field, and the viewing angle and mass-radius relation of the neutron star. One of our tools for this is a code (Chen & Shaham 1989) which takes into

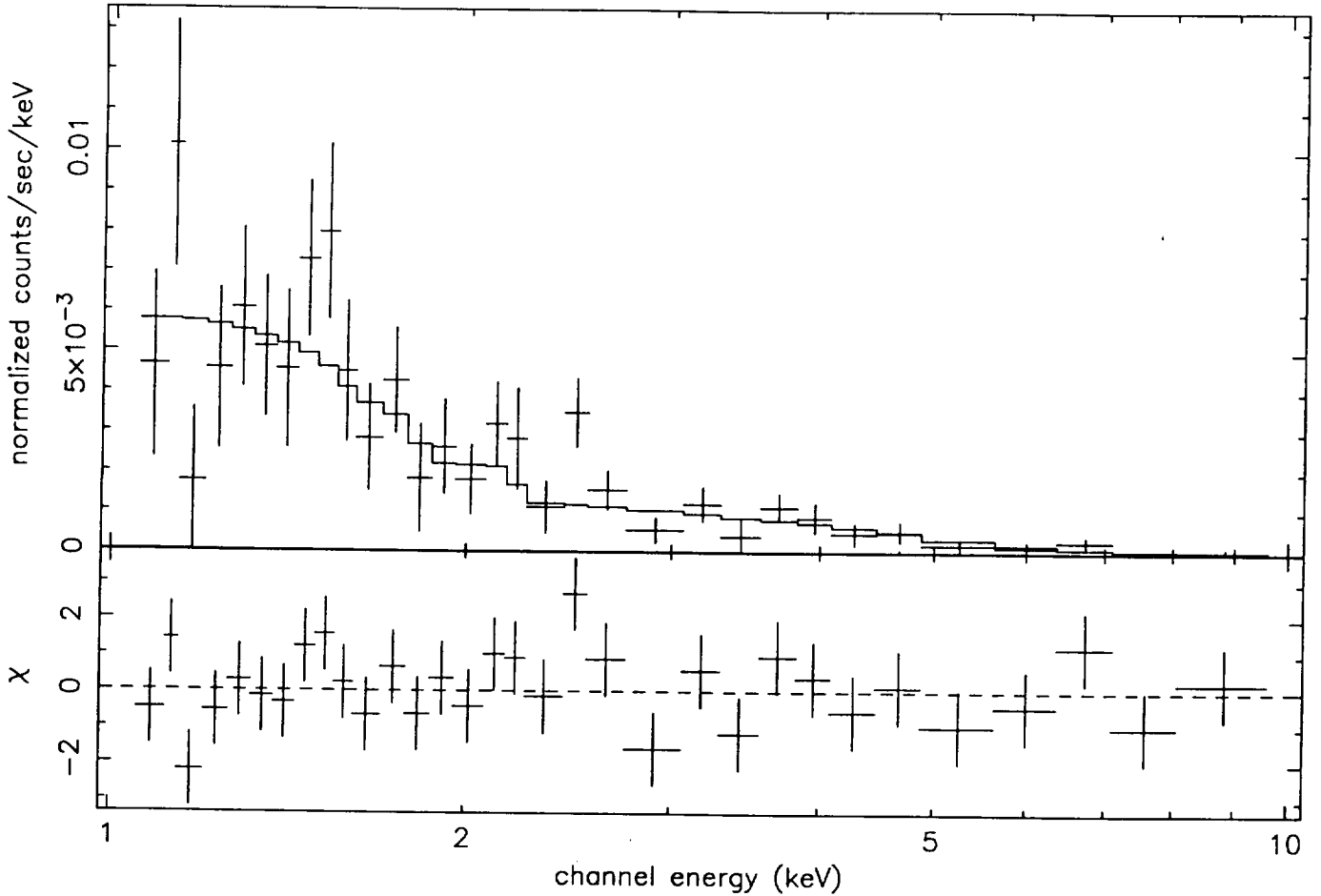


FIG. 3.— Power-law fit to the SIS0 spectrum of Geminga. The fitted photon index is  $1.56 \pm 0.17$ .

account all relativistic effects for spots of arbitrary size and viewing geometry. In particular, *we will test our theory that the single-peaked X-ray pulse, in combination with the double-peaked  $\gamma$ -ray pulse, means that the surface magnetic field has a sunspot geometry.*

We are in the process of analyzing the spectra from all four instruments. Preliminary results show that Geminga is detected up to 5 keV, and that the spectra can be fitted by either blackbody or power-law models. However, the blackbody result is somewhat implausible because at a fitted temperature of  $8 \times 10^6$  K, the emitting spot would have a radius of only 7 meters. Instead, the power-law fits to the SIS and the GIS (Figures 3 and 4,

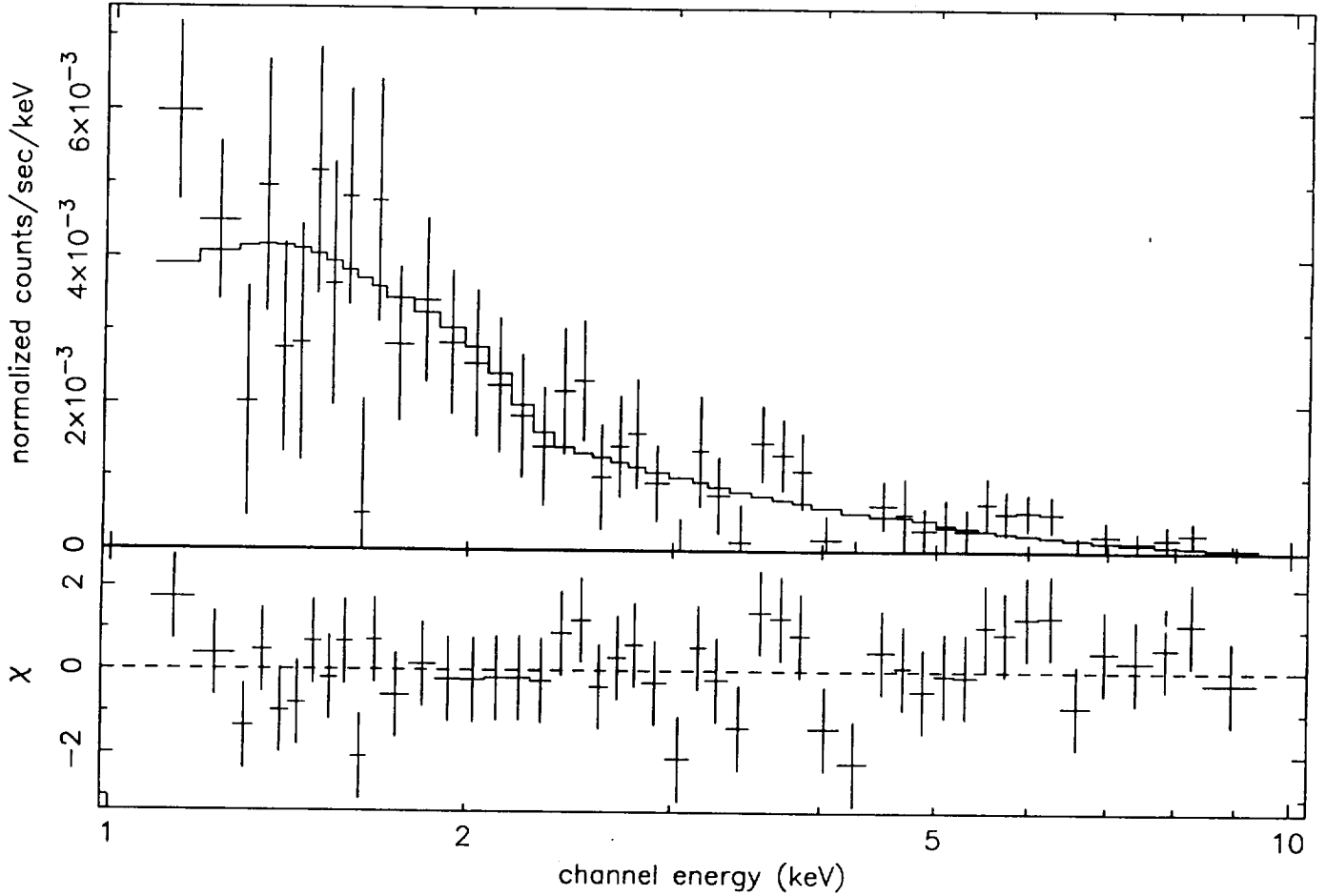


FIG. 4.— Power-law fit to the GIS3 spectrum of Geminga. The fitted photon index is  $2.14 \pm 0.31$ .

respectively), indicate probable nonthermal emission with a photon index of approximately 1.5.

The next step in the analysis will be to fit the *ASCA* and *ROSAT* data simultaneously. Following that, we will also produce pulse profiles at at 0.237 s rotation period of Geminga from the GIS data, and compare them to the *ROSAT* and EGRET light curves.

### 3. Warm Absorbers: The Moment of Truth

The goal of this AO-1 observation was to obtain a high signal-to-noise ratio spectrum of the Seyfert galaxy NGC 3516, an object which we expected to be one of the best



candidates for a successful demonstration of the details of the warm-absorber model for the following reasons:

- (a) NGC 3516 has one of the most complex and variable X-ray spectra among Seyfert galaxies. In the *Einstein* IPC, two observations taken six months apart showed an increase by a factor of five in the 0.2–4.0 keV flux (Kruker, Urry, & Canizares 1990), accompanied by a large change in spectral slope. Although the IPC spectra were fitted with  $N_{\text{H}} < 3 \times 10^{20} \text{ cm}^{-2}$ , the simultaneous MPC spectra were characterized by a decrease in  $N_{\text{H}}$  from  $\sim 2 \times 10^{23}$  to  $\sim 5 \times 10^{22}$  (Halpern 1982). The *EXOSAT* ME measured a column density of  $\sim 2 \times 10^{22}$ , intermediate between the *Einstein* IPC and MPC values, and found a soft excess in the LE detector (Ghosh & Soundararajaperumal 1991).
- (b) In “modern” times, we measured the column density with great precision using *Ginga*, finding  $N_{\text{H}} = (4.0 \pm 0.3) \times 10^{22}$  (Kolman *et al.* 1993). But then a *ROSAT* PSPC observation showed the X-ray flux to be in the highest state ever recorded, with  $N_{\text{H}} < 3 \times 10^{20}$ , consistent with the Galactic value. The fact that these reliably measured column densities differ by more than a factor of 100 is a sure sign that a warm absorber is implicated. More direct evidence for the warm absorber comes from the details of the *Ginga* and *ROSAT* spectra. First, the *Ginga* spectrum is poorly described by a power law or a partial covering model, and much better fitted by a warm iron edge with ionization stage between  $\text{Fe}^{+12}$  and  $\text{Fe}^{+21}$ . The effective column density of the warm absorber is  $\sim 3 \times 10^{23}$ . (A reflection model is unable to fit this spectrum with a reasonable value of the reflected fraction and spectral index.) Finally, a power-law fit to the *ROSAT* spectrum 2) shows marked deviations, most notably a dip at 0.9 keV which is the classic signature of a warm absorber.
- (c) A compilation of all the historical X-ray data on NGC 3516 shows that the apparent column density is inversely correlated with flux normalization, an indication that the variation in column density is not random, but is controlled by the strength of the

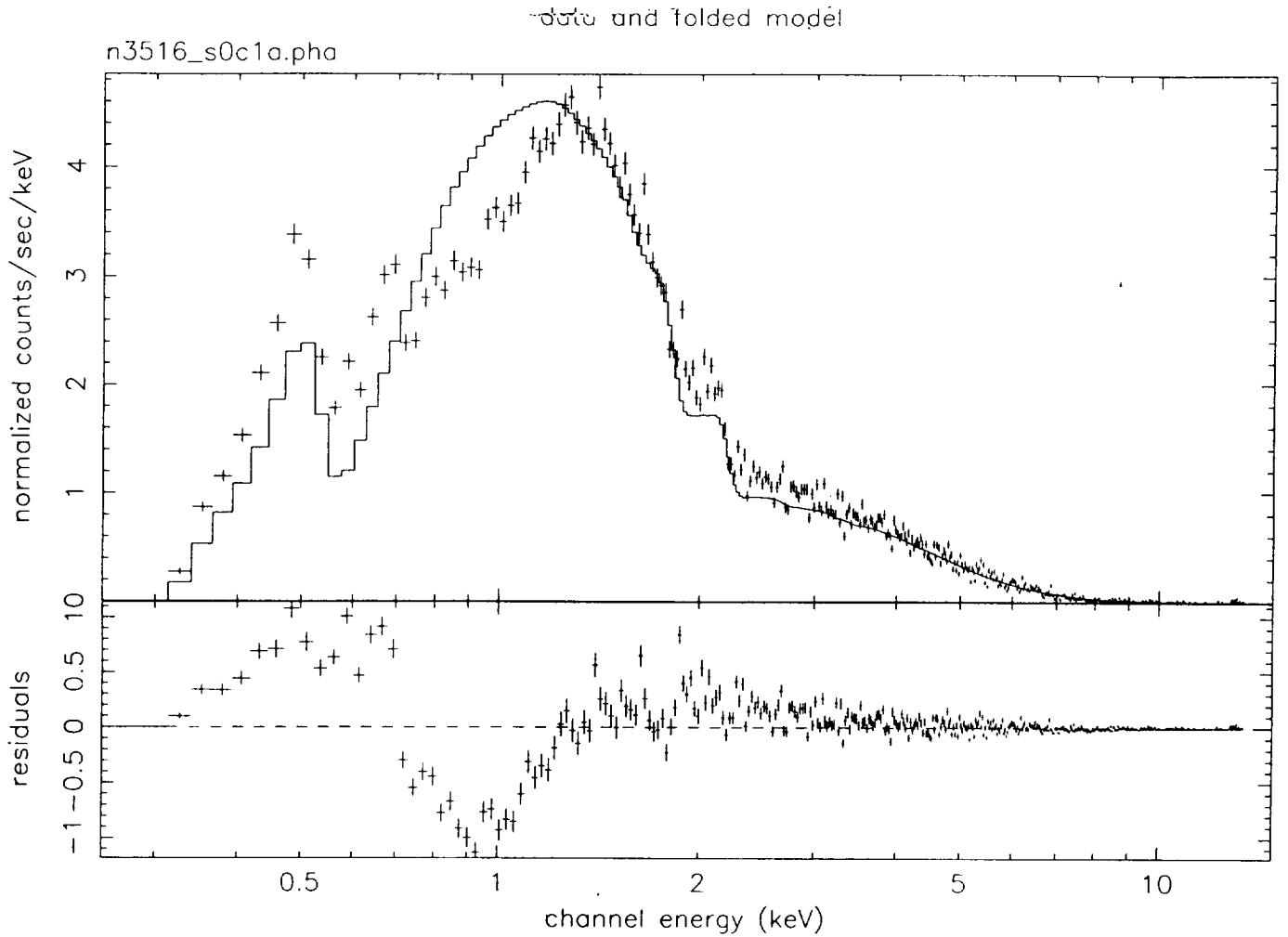


FIG. 5.— Power-law fit to the SIS0 spectrum of NGC 3516 showing strong residuals from a warm oxygen absorber.

X-ray continuum. Detailed calculations have shown that a change in ionizing flux of only a factor of three is sufficient to cause an apparent change in  $N_{\text{H}}$  of a factor of 100, as inferred by (incorrectly) fitting a neutral absorber (Halpern 1984; Netzer 1993).

The actual spectrum obtained of NGC 3156 shows all of the predicted features spectacularly, including the edges of  $\text{O}^{+6}$  at 739 eV and  $\text{O}^{+7}$  at 870 eV. Figure 5 is a fit of a simple power law to the SIS0 data. Obviously, there is a great deal of complex structure in this spectrum, and we will continue to analyze it, in combination with our *ROSAT* spectrum that shows similar features, albeit at lower resolution.

## REFERENCES

- Arons, J. 1981, *Ap. J.*, **248**, 1099.
- Bertsch, D. L., et al. 1992, *Nature*, **357**, 306.
- Boller, T., et al. 1992, *Astr. Ap.*, **261**, 57.
- Boller, T., et al. 1993, *Astr. Ap.*, **279**, 53.
- Brandt, W. N., et al. 1994, *M.N.R.A.S.*, **271**, 958.
- Brandt, W. N., et al. 1995, *M.N.R.A.S.*, **273**, L47.
- Chen, K. & Shaham, J. 1989, *Ap. J.*, **339**, 279.
- Elizalde, F., & Steiner, J. E. 1994, *M.N.R.A.S.*, **268**, L47.
- Ghosh, K. K., & Soundararajaperumal 1991, *Ap. J.*, **383**, 574.
- Grupe, D., et al. 1995, *Astr. Ap.*, **299**, L5.
- Halpern, J. P. 1982, Ph.D. thesis, Harvard University.
- Halpern, J. P. 1984, *Ap. J.*, **281**, 90.
- Halpern, J. P., & Holt, S. S. 1992, *Nature*, **357**, 222.
- Halpern, J. P., & Ruderman, M. 1993, *Ap. J.*, **415**, 286.
- Harding, A. K., Ozeroy, L. M., & Usov, V. V. 1993, *M.N.R.A.S.*, **265**, 921.
- Kolman, M., Halpern, J.P., Martin, C., Awaki, H., & Koyama, K. 1993, *Ap. J.*, **403**, 592.
- Kruper, J., Urry, C. M., & Canizares, C. 1990, *Ap. J. Suppl.*, **74**, 347.
- Moran, E. C., Halpern, J. P., & Helfand, D. J. 1994, *Ap. J. (Letters)*, **433**, L65.
- Moran, E. C., Halpern, J. P., & Helfand, D. J. 1996, *Ap. J. Suppl.*, in press.
- Netzer, H. 1993, *Ap. J.*, **411**, 594.
- Phillips, M. M. 1976, *Ap. J.*, **208**, 37.
- Remillard, R. A., et al. 1986, *Ap. J.* **301**, 742.
- Remillard, R. A., et al. 1991, *Nature*, **350**, 589.
- Ruderman, M., & Sutherland, P. G. 1975, *Ap. J.*, **196**, 57.